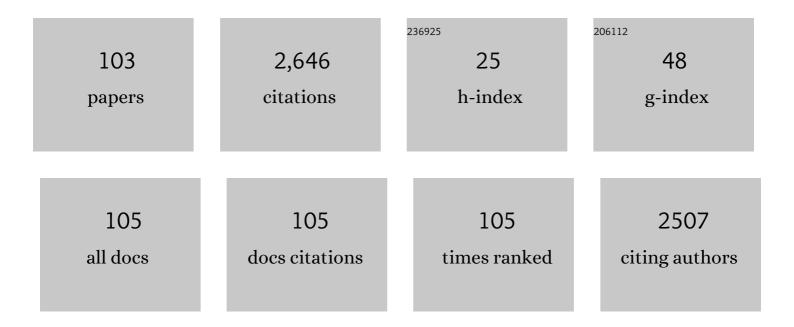
## Naoki Terada

List of Publications by Year in descending order

Source: https://exaly.com/author-pdf/328182/publications.pdf Version: 2024-02-01



Νλοκι Τερλολ

#	Article	IF	CITATIONS
1	The Mars system revealed by the Martian Moons eXploration mission. Earth, Planets and Space, 2022, 74, .	2.5	11
2	Martian moons exploration MMX: sample return mission to Phobos elucidating formation processes of habitable planets. Earth, Planets and Space, 2022, 74, .	2.5	51
3	Modeling of Diffuse Auroral Emission at Mars: Contribution of MeV Protons. Journal of Geophysical Research: Space Physics, 2022, 127, .	2.4	10
4	Effect of Meteoric Ions on Ionospheric Conductance at Jupiter. Journal of Geophysical Research: Space Physics, 2022, 127, .	2.4	6
5	Variations in Vertical CO/CO <sub>2</sub> Profiles in the Martian Mesosphere and Lower Thermosphere Measured by the ExoMars TGO/NOMAD: Implications of Variations in Eddy Diffusion Coefficient. Geophysical Research Letters, 2022, 49, .	4.0	7
6	Formation Mechanisms of the Molecular Ion Polar Plume and Its Contribution to Ion Escape From Mars. Journal of Geophysical Research: Space Physics, 2022, 127, .	2.4	4
7	Multispecies MHD Study of Ion Escape at Ancient Mars: Effects of an Intrinsic Magnetic Field and Solar XUV Radiation. Journal of Geophysical Research: Space Physics, 2022, 127, .	2.4	2
8	Effects of the IMF Direction on Atmospheric Escape From a Marsâ€like Planet Under Weak Intrinsic Magnetic Field Conditions. Journal of Geophysical Research: Space Physics, 2021, 126, e2020JA028485.	2.4	8
9	Stability of Atmospheric Redox States of Early Mars Inferred from Time Response of the Regulation of H and O Losses. Astrophysical Journal, 2021, 912, 135.	4.5	6
10	Intense Zonal Wind in the Martian Mesosphere During the 2018 Planetâ€Encircling Dust Event Observed by Groundâ€Based Infrared Heterodyne Spectroscopy. Geophysical Research Letters, 2021, 48, e2021GL092413.	4.0	4
11	Pre-flight Calibration and Near-Earth Commissioning Results of the Mercury Plasma Particle Experiment (MPPE) Onboard MMO (Mio). Space Science Reviews, 2021, 217, 1.	8.1	32
12	Global climate and river transport simulations of early Mars around the Noachian and Hesperian boundary. Icarus, 2021, 368, 114618.	2.5	16
13	Mars' atmospheric neon suggests volatile-rich primitive mantle. Icarus, 2021, 370, 114685.	2.5	7
14	Seasonal and Dustâ€Related Variations in the Dayside Thermospheric and Ionospheric Compositions of Mars Observed by MAVEN/NGIMS. Journal of Geophysical Research E: Planets, 2021, 126, e2021JE006926.	3.6	8
15	Surface environment of Phobos and Phobos simulant UTPS. Earth, Planets and Space, 2021, 73, .	2.5	15
16	In situ observations of ions and magnetic field around Phobos: the mass spectrum analyzer (MSA) for the Martian Moons eXploration (MMX) mission. Earth, Planets and Space, 2021, 73, .	2.5	14
17	Science operation plan of Phobos and Deimos from the MMX spacecraft. Earth, Planets and Space, 2021, 73, .	2.5	22
18	A coupled atmosphere–hydrosphere global climate model of early Mars: A â€~cool and wet' scenario for the formation of water channels. Icarus, 2020, 338, 113567.	2.5	24

#	Article	IF	CITATIONS
19	Vertical Propagation of Wave Perturbations in the Middle Atmosphere on Mars by MAVEN/IUVS. Journal of Geophysical Research E: Planets, 2020, 125, e2020JE006481.	3.6	18
20	Statistical study of non-adiabatic energization and transport in Kelvin-Helmholtz vortices at mercury. Planetary and Space Science, 2020, 193, 105079.	1.7	4
21	Martian Oxygen and Hydrogen Upper Atmospheres Responding to Solar and Dust Storm Drivers: Hisaki Space Telescope Observations. Journal of Geophysical Research E: Planets, 2020, 125, e2020JE006500.	3.6	6
22	MESSENGER Observations of Planetary Ion Characteristics in the Vicinity of Kelvinâ€Helmholtz Vortices at Mercury. Journal of Geophysical Research: Space Physics, 2020, 125, e2020JA027871.	2.4	3
23	Seasonal and Latitudinal Variations of Dayside N <sub>2</sub> /CO <sub>2</sub> Ratio in the Martian Thermosphere Derived From MAVEN IUVS Observations. Journal of Geophysical Research E: Planets, 2020, 125, e2020JE006378.	3.6	8
24	Impact-induced amino acid formation on Hadean Earth and Noachian Mars. Scientific Reports, 2020, 10, 9220.	3.3	25
25	A Warm Layer in the Nightside Mesosphere of Mars. Geophysical Research Letters, 2020, 47, e2019GL085646.	4.0	9
26	Effects of an Intrinsic Magnetic Field on Ion Loss From Ancient Mars Based on Multispecies MHD Simulations. Journal of Geophysical Research: Space Physics, 2020, 125, e2019JA026945.	2.4	24
27	Vertical Coupling Between the Cloud‣evel Atmosphere and the Thermosphere of Venus Inferred From the Simultaneous Observations by Hisaki and Akatsuki. Journal of Geophysical Research E: Planets, 2020, 125, e2019JE006192.	3.6	2
28	Design for stray-light reduction to a Martian ionospheric imager. Applied Optics, 2020, 59, 9937.	1.8	0
29	Suzaku detection of enigmatic geocoronal solar wind charge exchange event associated with coronal mass ejection. Publication of the Astronomical Society of Japan, 2019, 71, .	2.5	10
30	Highly Oxidizing Aqueous Environments on Early Mars Inferred From Scavenging Pattern of Trace Metals on Manganese Oxides. Journal of Geophysical Research E: Planets, 2019, 124, 1282-1295.	3.6	19
31	Sodium Ion Dynamics in the Magnetospheric Flanks of Mercury. Geophysical Research Letters, 2018, 45, 595-601.	4.0	10
32	Study of the Transition from MRI to Magnetic Turbulence via Parasitic Instability by a High-order MHD Simulation Code. Astrophysical Journal, 2018, 853, 174.	4.5	5
33	Effects of a Weak Intrinsic Magnetic Field on Atmospheric Escape From Mars. Geophysical Research Letters, 2018, 45, 9336-9343.	4.0	29
34	Loss of the Martian atmosphere to space: Present-day loss rates determined from MAVEN observations and integrated loss through time. Icarus, 2018, 315, 146-157.	2.5	216
35	High-contrast apodization baffle for instruments onboard solar system exploration missions. , 2018, ,		1
36	Dawn-dusk difference of periodic oxygen EUV dayglow variations at Venus observed by Hisaki. Icarus, 2017, 292, 102-110.	2.5	7

#	Article	IF	CITATIONS
37	MAVEN NGIMS observations of atmospheric gravity waves in the Martian thermosphere. Journal of Geophysical Research: Space Physics, 2017, 122, 2310-2335.	2.4	88
38	Planetary plasma and atmospheres explored by space missions in Japan: Hisaki, Akatsuki, and beyond. Journal of Physics: Conference Series, 2017, 869, 012094.	0.4	0
39	Global distribution and parameter dependences of gravity wave activity in the Martian upper thermosphere derived from MAVEN/NGIMS observations. Journal of Geophysical Research: Space Physics, 2017, 122, 2374-2397.	2.4	66
40	A fullâ€particle Martian upper thermosphereâ€exosphere model using the DSMC method. Journal of Geophysical Research E: Planets, 2016, 121, 1429-1444.	3.6	5
41	Comparison of the Martian thermospheric density and temperature from IUVS/MAVEN data and general circulation modeling. Geophysical Research Letters, 2016, 43, 3095-3104.	4.0	34
42	Periodic variations of oxygen EUV dayglow in the upper atmosphere of Venus: Hisaki/EXCEED observations. Journal of Geophysical Research E: Planets, 2015, 120, 2037-2052.	3.6	14
43	Harmonics of whistler-mode waves near the Moon. Earth, Planets and Space, 2015, 67, 36.	2.5	9
44	Field-of-View Guiding Camera on the HISAKI (SPRINT-A) Satellite. Space Science Reviews, 2014, 184, 259-274.	8.1	46
45	Extreme Ultraviolet Radiation Measurement for Planetary Atmospheres/Magnetospheres from the Earth-Orbiting Spacecraft (Extreme Ultraviolet Spectroscope for Exospheric Dynamics: EXCEED). Space Science Reviews, 2014, 184, 237-258.	8.1	68
46	Groupâ€standing of whistler mode waves near the Moon. Journal of Geophysical Research: Space Physics, 2014, 119, 2634-2648.	2.4	5
47	Inner heliosphere MHD modeling system applicable to space weather forecasting for the other planets. Space Weather, 2014, 12, 187-204.	3.7	68
48	Reduction of the fieldâ€aligned potential drop in the polar cap during large geomagnetic storms. Journal of Geophysical Research: Space Physics, 2013, 118, 4864-4874.	2.4	6
49	Estimation of the permittivity and porosity of the lunar uppermost basalt layer based on observations of impact craters by SELENE. Journal of Geophysical Research E: Planets, 2013, 118, 1453-1467.	3.6	27
50	A simulation study of Ioâ€related Jovian decametric radiation: Control factor of occurrence probability. Journal of Geophysical Research: Space Physics, 2013, 118, 5082-5098.	2.4	0
51	Suzaku Observation of Strong Solar-Wind Charge-Exchange Emission from the Terrestrial Exosphere during a Geomagnetic Storm. Publication of the Astronomical Society of Japan, 2013, 65, .	2.5	24
52	EFFECT OF BACKGROUND MAGNETIC FIELD ON TURBULENCE DRIVEN BY MAGNETOROTATIONAL INSTABILITY IN ACCRETION DISKS. Astrophysical Journal, 2013, 767, 165.	4.5	4
53	Dependence of O <sup>+</sup> escape rate from the Venusian upper atmosphere on IMF directions. Geophysical Research Letters, 2013, 40, 1682-1685.	4.0	39
54	Effects of the surface conductivity and the IMF strength on the dynamics of planetary ions in Mercury's magnetosphere. Journal of Geophysical Research: Space Physics, 2013, 118, 3233-3242.	2.4	15

#	Article	IF	CITATIONS
55	A simulation study of the currentâ€voltage relationship of the Io tail aurora. Journal of Geophysical Research, 2012, 117, .	3.3	10
56	Stormâ€ŧime electron density enhancement in the cleft ion fountain. Journal of Geophysical Research, 2012, 117, .	3.3	6
57	Statistical study of broadband whistlerâ€mode waves detected by Kaguya near the Moon. Geophysical Research Letters, 2012, 39, .	4.0	22
58	Centrifugally stimulated exospheric ion escape at Mercury. Geophysical Research Letters, 2012, 39, .	4.0	14
59	Photoelectron flows in the polar wind during geomagnetically quiet periods. Journal of Geophysical Research, 2012, 117, .	3.3	26
60	Suzaku observations of charge exchange emission from solar system objects. Astronomische Nachrichten, 2012, 333, 319-323.	1.2	1
61	Vertical connection from the tropospheric activities to the ionospheric longitudinal structure simulated by a new Earth's whole atmosphere-ionosphere coupled model. Journal of Geophysical Research, 2011, 116, n/a-n/a.	3.3	109
62	Solar zenith angle dependence of plasma density and temperature in the polar cap ionosphere and low-altitude magnetosphere during geomagnetically quiet periods at solar maximum. Journal of Geophysical Research, 2011, 116, n/a-n/a.	3.3	32
63	O <sup>+</sup> outflow channels around Venus controlled by directions of the interplanetary magnetic field: Observations of high energy O <sup>+</sup> ions around the terminator. Journal of Geophysical Research, 2011, 116, n/a-n/a.	3.3	22
64	An EUV spectrometer on earth-orbiting satellite for planetary science. Proceedings of SPIE, 2011, , .	0.8	0
65	Solar system planets observed with Suzaku. Advances in Space Research, 2011, 47, 411-418.	2.6	5
66	X-Ray Observation of Mars at Solar Minimum with Suzaku. Publication of the Astronomical Society of Japan, 2011, 63, S705-S712.	2.5	5
67	Vlasov simulation of the interaction between the solar wind and a dielectric body. Physics of Plasmas, 2011, 18, 012908.	1.9	20
68	Statistical analysis of monochromatic whistler waves near the Moon detected by Kaguya. Annales Geophysicae, 2011, 29, 889-893.	1.6	24
69	Enhancement of Terrestrial Diffuse X-Ray Emission Associated with Coronal Mass Ejection and Geomagnetic Storm. Publication of the Astronomical Society of Japan, 2011, 63, S691-S704.	2.5	26
70	The role of the electron convection term for the parallel electric field and electron acceleration in MHD simulations. Physics of Plasmas, 2011, 18, .	1.9	1
71	Earth-orbiting extreme ultraviolet spectroscopic imaging mission for planetary space science. , 2010, , .		0
72	DISCOVERY OF DIFFUSE HARD X-RAY EMISSION AROUND JUPITER WITH <i>SUZAKU</i> . Astrophysical Journal Letters, 2010, 709, L178-L182.	8.3	22

#	Article	IF	CITATIONS
73	A comparison of global models for the solar wind interaction with Mars. Icarus, 2010, 206, 139-151.	2.5	108
74	Time Variability of the Geocoronal Solar-Wind Charge Exchange in the Direction of the Celestial Equator. Publication of the Astronomical Society of Japan, 2010, 62, 981-986.	2.5	34
75	EUV spectroscopic imaging observations of the first mission of Japanese small scientific satellites series. Proceedings of SPIE, 2010, , .	0.8	1
76	Observations of veryâ€lowâ€energy (<10 eV) ion outflows dominated by O <sup>+</sup> ions in the region of enhanced electron density in the polar cap magnetosphere during geomagnetic storms. Journal of Geophysical Research, 2010, 115, .	3.3	23
77	Asymmetrical features of frequency and intensity in the Ioâ€related Jovian decametric radio sources: Modeling of the Ioâ€Jupiter system. Journal of Geophysical Research, 2010, 115, .	3.3	2
78	The HLLD Approximate Riemann Solver for Magnetospheric Simulation. IEEE Transactions on Plasma Science, 2010, 38, 2236-2242.	1.3	18
79	Comparative Study of Global MHD Simulations of the Terrestrial Magnetosphere With Different Numerical Schemes. IEEE Transactions on Plasma Science, 2010, 38, 2229-2235.	1.3	0
80	Performance Measurement of Magnetohydrodynamic Code for Space Plasma on the Various Scalar-Type Supercomputer Systems. IEEE Transactions on Plasma Science, 2010, 38, 2254-2259.	1.3	5
81	Atmosphere and Water Loss from Early Mars Under Extreme Solar Wind and Extreme Ultraviolet Conditions. Astrobiology, 2009, 9, 55-70.	3.0	86
82	Dynamics of magnetospheric ions at Mercury : some open questions awaiting Bepi Colombo measurements. , 2009, , .		0
83	MHD and Kinetic Modeling of the Ionospheres of Venus and Mars. , 2009, , .		0
84	Hybrid simulations of the O+ ion escape from Venus: Influence of the solar wind density and the IMF x component. Advances in Space Research, 2009, 43, 1436-1441.	2.6	16
85	Solarâ€wind control of the hot oxygen corona around Mars. Journal of Geophysical Research, 2009, 114, .	3.3	9
86	A threeâ€dimensional, multispecies, comprehensive MHD model of the solar wind interaction with the planet Venus. Journal of Geophysical Research, 2009, 114, .	3.3	44
87	Hermean Magnetosphere-Solar Wind Interaction. Space Sciences Series of ISSI, 2008, , 347-368.	0.0	3
88	Numerical Calculation on a Top-Hat Plasma Particle Analyzer Using a Boundary-Fitted Coordinate System. IEEE Transactions on Plasma Science, 2007, 35, 1178-1183.	1.3	1
89	Coronal Mass Ejection (CME) Activity of Low Mass M Stars as An Important Factor for The Habitability of Terrestrial Exoplanets. II. CME-Induced Ion Pick Up of Earth-like Exoplanets in Close-In Habitable Zones. Astrobiology, 2007, 7, 185-207.	3.0	256
90	Time variation of nonthermal escape of oxygen from Mars after solar wind dynamic pressure enhancement. Geophysical Research Letters, 2007, 34, .	4.0	11

#	Article	IF	CITATIONS
91	Ion energization during substorms at Mercury. Planetary and Space Science, 2007, 55, 1502-1508.	1.7	16
92	Hermean Magnetosphere-Solar Wind Interaction. Space Science Reviews, 2007, 132, 529-550.	8.1	48
93	Effect of the motional electric field on the Venus nightside ionopause. Journal of Geophysical Research, 2006, 111, .	3.3	1
94	Atmospheric and water loss from early Venus. Planetary and Space Science, 2006, 54, 1425-1444.	1.7	120
95	Terrestrial nitrogen and noble gases in lunar soils. Nature, 2005, 436, 655-659.	27.8	99
96	A comparison of magnetohydrodynamic instabilities at the Martian ionopause. Advances in Space Research, 2005, 36, 2049-2056.	2.6	16
97	Electron dynamics during substorm dipolarization in Mercury's magnetosphere. Annales Geophysicae, 2005, 23, 3389-3398.	1.6	23
98	Global hybrid model of the solar wind interaction with the Venus ionosphere: ion escape processes. Advances in Space Research, 2004, 33, 161-166.	2.6	28
99	EUV imaging of near-Venus space. Advances in Space Research, 2004, 33, 1932-1937.	2.6	8
100	Global hybrid simulation of the Kelvin-Helmholtz instability at the Venus ionopause. Journal of Geophysical Research, 2002, 107, SMP 30-1-SMP 30-20.	3.3	130
101	Unsteady behavior of supercritical perpendicular shock waves in a multiple-ion-species plasma. Advances in Space Research, 1999, 24, 113-116.	2.6	3
102	Storm-time magnetic field variations observed by the ETS-VI satellite. Earth, Planets and Space, 1998, 50, 853-864.	2.5	17
103	EXTREME ULTRAVIOLET SPECTROSCOPE FOR EXOSPHERIC DYNAMICS EXPLORE (EXCEED). , 0, , 579-591.		2